ISSN: 2230-9926

Available online at http://www.journalijdr.com

IJDR

International Journal of Development Research
Vol. 10, Issue, 06, pp. 36776-36781, June, 2020
https://doi.org/10.37118/ijdr.19040.06.2020

RESEARCH ARTICLE OPEN ACCESS

BROADBAND PATCH ANTENNAS BIO-INSPIRED IN THE ELLIPTICAL LEAF DEVELOPED WITH THE RIEMANN TRANSFORMATION FOR WLAN AND 5G APPLICATIONS

***[1]Tales A. C. de Barros, Paulo H. F. Silva, [1]Lamarks T. C. Cavalcanti, [2]Rodrigo C. F. da Silva, [2]Pedro Carlos de Assis Júnior, [3]Paulo F. Silva Junior, [3]Ewaldo E. C. Santana and [4]Elder Eldervitch Carneiro de Oliveira**

[1]Electrical Engineering Department, Federal Institute of Paraíba, João Pessoa – PB, Brasil
[2]Phisics department, State University of Paraíba, Patos – PB, Brasil
[3]Graduate of Computer Engineeringand Systems, University State of Maranhão, São Luís – MA, Brasil
[4]CCBSA Center, State University of Paraíba, João Pessoa – PB, Brasil

ARTICLE INFO

Article History:
Received 17th March, 2020
Received in revised form
08th April, 2020
Accepted 06th May, 2020
Published online 29th June, 2020

Key Words:

CAD, Conformal mapping,
Broadband antennas,
Microstrip patch antennas,
Wireless applications.

****Corresponding author: Tales A. C. de Barros,***

ABSTRACT

This paper describes the development of broadband patch antennas using Riemann conformal transformation, on the square in the Argand-Gauss plane for wireless local area network (2.4 GHz and 5 GHz), and 5G band in 3.5 GHz. For this work was projected three antennas with the bio-inspired shape of the elliptical leaf(MPA R1, MPA R2, and MPA R3), using Riemann conformal transformation, for an increase of the bandwidth of the narrowband antenna (square patch antenna), fractional bandwidth of 3%, to broadband antennas, with fractional bandwidth greater than 5%. The project of the antennas was generated in MATLAB, simulated in the commercial software ANSYS, and built in low-cost material, fiberglass dielectric substrate. The measured results of the bio-inspired antennas patch antennas, with Riemann transformation, operation in the 2.4 GHz, 3.5 GHz and 5.8 GHz bands, with absolute bandwidth of 135 MHz (MPA R1), 220 MHz (MPA R2) and 440 MHz (MPA R3), fractal bandwidth of 5.6% (MPA R1), 220 MHz 6.3%(MPA R2) and 440 MHz 7.6%(MPA R3), the simulated maximum gain of 6.67 dBi (MPA R1), and a half-power beamwidth of 108 degrees (MPA R2).

Citation: ***Tales A. C. de Barros, Paulo H. F. Silva, Lamarks T. C. Cavalcanti, Rodrigo C. F. da Silva, Pedro Carlos de Assis Júnior et al.*** "Broadband patch antennas bio-inspired in the elliptical leaf developed with the riemann transformation for wlan and 5g applications*", International Journal of Development Research*, 10, (06), 36776-36781.

INTRODUCTION

The microstrip patch antennas (MPA) have characteristics of construction and operation that have been widely used in several civil and military applications (Kumar *et al*., 2003). In terms of operation, a conventional MPA antenna features a broadside radiation diagram with a good beam width, with a directional gain of around 6 dBi, with resonant properties of a narrowband antenna, with a percentage bandwidth between 1% and 3%, as (Balanis, 1997; Chen *et al*., 2005). These characteristics, reduced the gain and narrow bandwidth, often limit its applications in wireless systems and devices. However, the gain of an MPA antenna can be increased, for example, with the use of an arrangement of these antennasaccording to (Stuzman and Thiele, 2013). A review of techniques used to increase the bandwidth of MPA antennas can be found in (Ajay *et al*., 2012), and include: the modified shape patch, multiresonator technique, multilayered technique and stacked multilayered technique. Using these techniques, one can easily obtain percentage bandwidths above 10% for modified MPA antennas. The broadband technique, which modifies the patch format, was chosen for this study because it preserves most of the characteristics and advantages of a conventional MPA antenna. Some examples, which use this approach, have been reported in the literature and include the use of conventional patches (rectangular and circular) with slits (Jui-Han Lu, 2003; Deshmukh *et al*., 2013; Jeffrey *et al*., 2016; Ata *et al*., 2018). Generally, the shapes of the slots are letters, E, H and U according to the works (Aravindraj *et al*., 2017; Nitin *et al*., 2018) and (Ibrahim, 2019), these are the most used formats for improving the bandwidth, as well as for multiband applications. Antennas with U-shaped slots and fed

by a probe can have percentage bandwidths between 11% and 43% (Khidre et al., 2013) and (Khan *et al*., 2018). The plant-shapes has been used in the development of several antenna types, as of patch, monopole, aperture-coupled, in wearable, on-chip, and other applications, built in rigid and flexible dielectric substrates as fiber-glass, polyamide, and acetate (Silva Junior, *et al*., 2019), (Silva Junior, *et al*., 2019), (Silva Junior, *et al*., 2020), (Silva Junior, *et al*., 2018), (Silva Junior, *et al*., 2016), (Silva Junior, *et al*., 2016). The advantage of the plant shape is that it has a great perimeter with compact structures, enabling the development of the small antennas operating in low frequencies. In this article, a broadband MPA antennausing a Riemann conformal transformation on square antenna, is developing, cover the 2.4 GHz, and 5.8 GHz, WLAN band according to the IEEE802.11 communication standards, and 3.5 GHz,5G bands.This work consists of three more sections in addition to this introduction. Section II presents the materials and methods used in the development of the work. In section III, are discussed the results obtained in the simulations and measurements of structures, and in section IV the final considerations are addressed.

MATERIALS AND METHODS

The microstrip patch antennas considered in this paper consist of a radiating conductive patch fed by a microstrip line and a finite conductive ground plane, which are separated by a thick dielectric substrate, h= 1.5 mm, as shown in Figure 1. The width of the Riemann patch, W_1 (mm), is equal to twice its length,$L_1 = \lambda_g/2$ (mm). The value of the guided wavelength, λ_g, is given by (1).

$$\lambda_g = c/f_r\sqrt{\varepsilon_r} \quad (1)$$

The Riemann patch is fed by a microstrip line divided into two sections of equal length ($L_2 = L_3$):

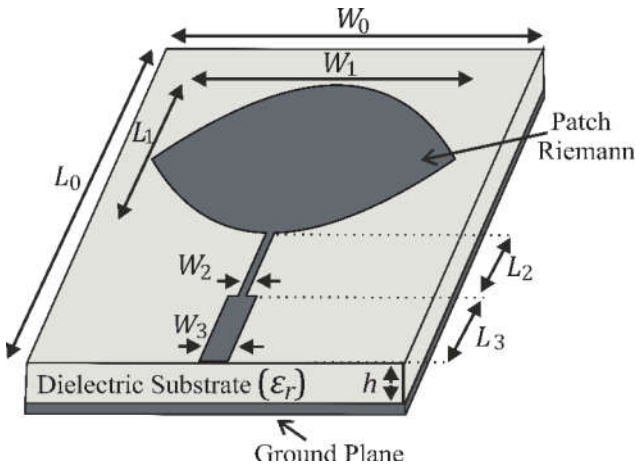

Figure 1. Microstrip patch Riemann Antenna

A 50 Ω pad line, in which an SMA connector is welded to connect a 50 Ω coaxial cable; and an quarter-wave transformer, whose function is to match the impedance of the 50 Ω line section (pad line) and the input impedance of the radiating Riemann patch. For each line section, the width (W_2 or W_3), in mm, is calculated and adjusted according to the desired impedance. The proposed antenna patch has a total area of W_0xL_0, in which:

$$W_0 = W_1 + 13.3h \quad (2)$$

$$L_0 = L_1 + L_2 + L_3 + 6.7h \quad (3)$$

The material chosen for the manufacture of the antennas was the fiber-glass (FR-4), whose thickness value of the dielectric substrate layer is h= 1.5mm, with relative electrical permittivity$\varepsilon_r = 4.4$ and a loss tangent of 0.02. The FR-4 is widely used in printed circuit technology and is suitable for low-cost and compact antennas designs, as it has inherent characteristics for applications in planar antennas. The microstrip antennas of type patch were designed using a radiating element model generated from a transformation conformal to Riemann, in a square in the Argand-Gauss plane.An example of transformed geometry, generated for the radiating element on MATLAB™, can be seen in Figure 2, where the expression (4) was used in the corresponding transformation.

$$f(z) = (z^2 - 1)^{1/2} \quad (4)$$

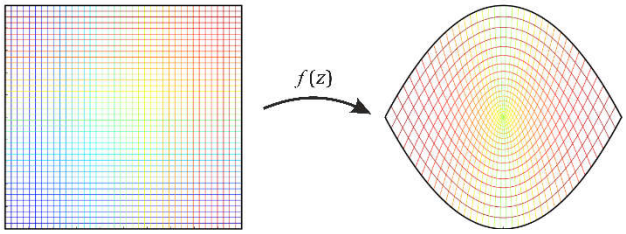

Figure 2. Example of transformation conformal (a) square, (b) Riemann square

With the application of Riemann's transformed geometry, three microstrip antennas of type patch were designed, named as: MPAR1, MPA R2 and MPA R3, with variation in the dimensions of widthW_1 and lengthL_1, to the adjusting at in resonance frequencies in 2.4 GHz, 3.5 GHz and 5.8 GHz. The shape chosen for the development of the work was that of an elliptical leaf, which can be observed in many types of plants. This shape was chosen for simplicity of the shape, and for its adaptation to the Riemann transformation, being able to be applied without additional modifications, taking advantage of the characteristics of the increase of the perimeter in a compact structure. The methodology adopted in this work, to obtain of the prototypes of type patch Riemann microstrip antennas, was carried out in stages, according to the flowchart of Figure 3.

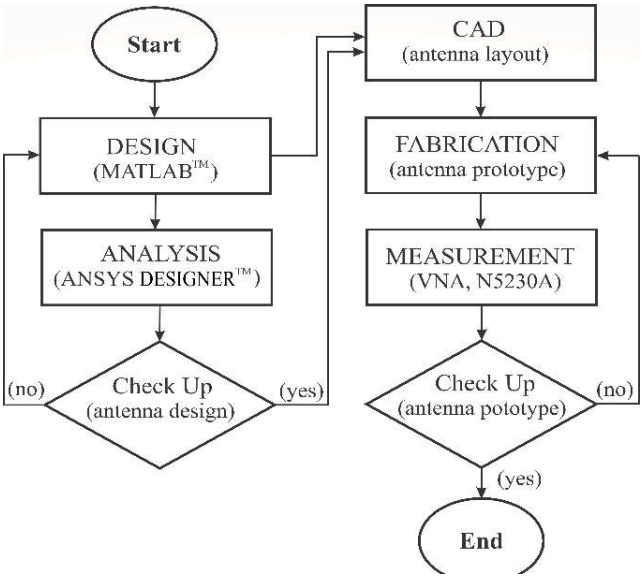

Figure 3. Flowchart of the methodology used in this work

For the feeding of the antennas was used the technique by microstrip line inserted directly in the radiating element and together with a quarter wave transformer, for the impedance matching. This feed technique is one of the easiest in terms of coupling and analysis, since its dimensions depend to frequency of resonance and the characteristic impedance of the power supply. The values antennas dimensions proposed are listed in Table 1.

Table 1. Dimensions of the designed antennas

Dimensions in mm	MPA R1	MPA R2	MPA R3
Width (W_0)	89.00	67.40	48.40
Width (W_1)	69.00	47.40	28.20
Width(W_2)	1.40	1.30	1.33
Width(W_3)	2.87	2.87	2.87
Length (L_0)	74.32	54.56	36.90
Length (L_1)	34.50	23.70	14.20
Length (L_2)	14.91	10.43	6.32
Length (L_3)	14.91	10.43	6.32

RESULTS AND DISCUSSION

Figure 4 shows the prototypes manufactured of the Riemann patch microstrip antennas, MPA R1, MPA R2 and MPA R3.

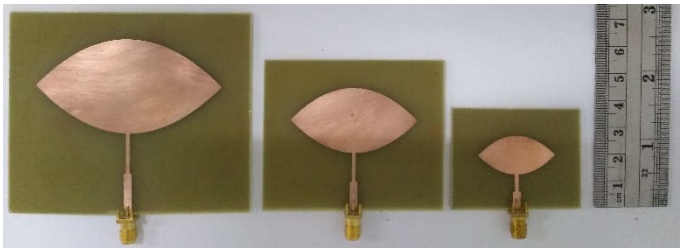

Figure 4. Antenna prototypes: MPA R1, MPA R2 and MPA R3

The parameter of the reflection coefficient module,S_{11}, of the projected antennas were simulated in the frequency range of 1.0 - 7.0 GHz, as observed in Figure 5. In the simulation was observed the results of the bandwidth (BW): MPA R1 = 111.25 MHz; MPA R2 = 180.00 MHz; and MPA R3 = 382.50 MHz. From the use of the quarter-wave transformer in the microstrip line, the antennas obtained a better reflection coefficient, S_{11} below of $-40{,}0$ dB in the central resonance frequencies(f_c), 2.39 GHz, 3.44 GHz and 5.63 GHz.

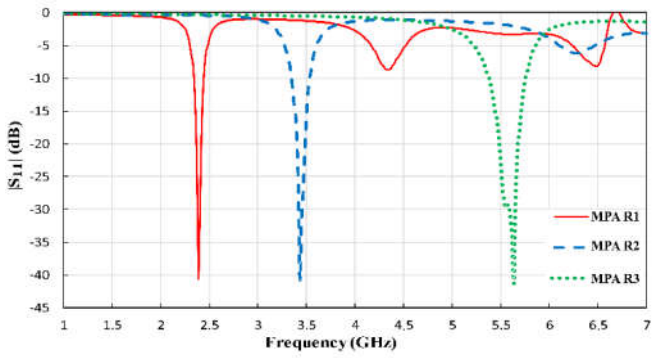

Figure 5. Comparison of the parameter simulated, $|S_{11}|$, of the antennas: MPA R1, MPA R2 and MPA R3

The simulation was performed in commercial software ANSYS™, and the measurements was performed in the measure's laboratory of the Federal Institute of Paraiba, Campus of Joao Pessoa, PB, with the VNA of Agilent Technology model E5071C (300 kHz–20 GHz). The results simulated in ANSYS™ of the parameter S_{11} were compared with VNA measurements. According to the values indicated in Table 2, the measurements of the parameters S_{11} in dB of theantennas:

MPA R1 = -28.90 dB, f_c of 2.45GHz;
MPA R2 = -33.60 dB,f_c of 3.46 GHz; and
MPA R3 = -31.98 dB,f_c of 3.71 GHz.

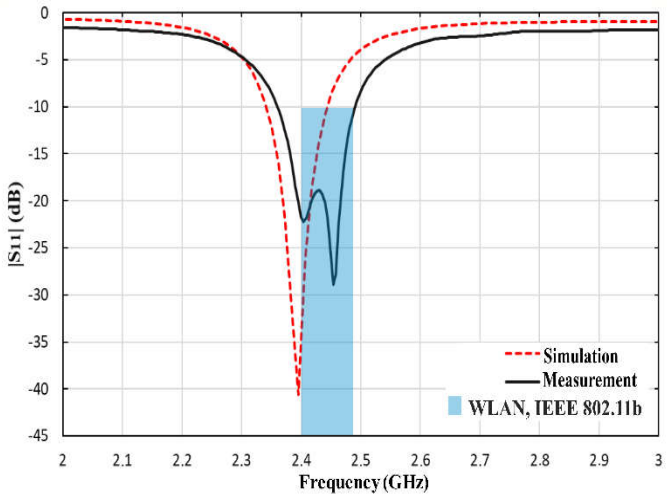

(a)

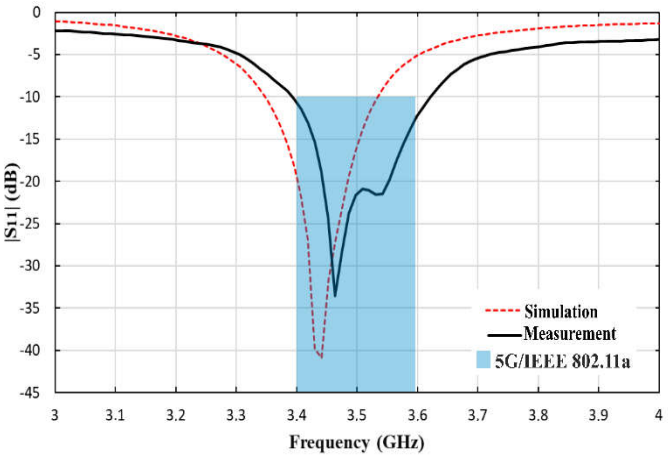

(b)

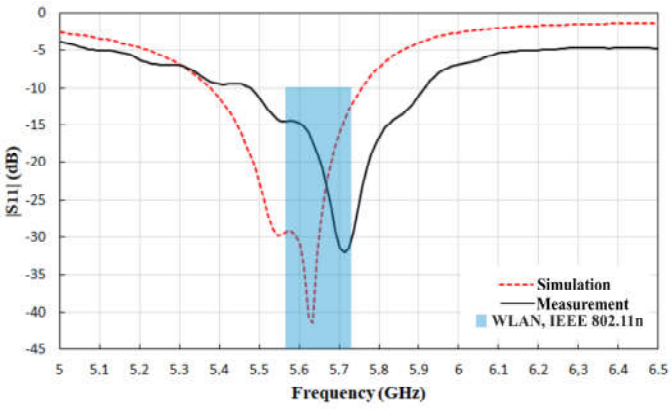

(c)

Figure 6. Comparison of the parameter, $|S_{11}|$, simulated and measured, of the antennas: (a) MPA R1, (b) MPA R2 and (c) MPA R3

Figure 6 shows the comparison of simulated and measured results of S_{11} parameters of MPA R1, MPA R2, and MPA R3, and the values can be observed in Table 2. Figure 6(a) illustrate the comparison of the simulation and measurement of

the parameter S_{11}, of the MPA R1, in 2.0 – 3.0 GHz frequency range. From the measured and simulated results, it can be indicated that the MPA R1 presents measured bandwidth of 135 MHz, with 21.34% greater than the simulated bandwidth, and error of 2.51% between simulated and measured resonance frequency(f_c). In the results of the MPA R2, Figure 6(b), it can be observed that the measured bandwidth is 440.0 MHz, 15% greater than the simulated bandwidth, and error of1.42% de between simulated and measured resonance frequency (f_c). The results of the MPA R3 can be observed in Figure 6(c), with the measured bandwidth of 220.0 MHz, 22.22% greater than the simulated bandwidth, anderror of 0.58% between simulated and measured resonance frequency (f_c).

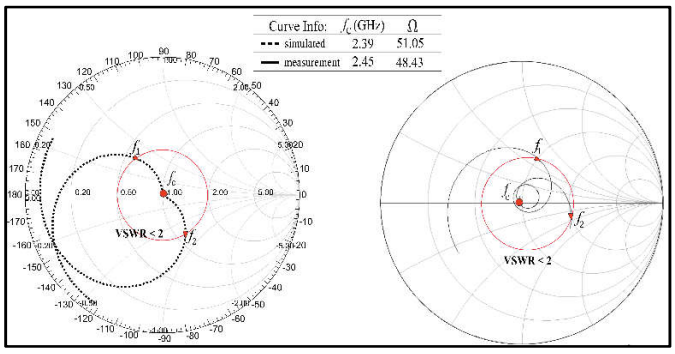

(a)

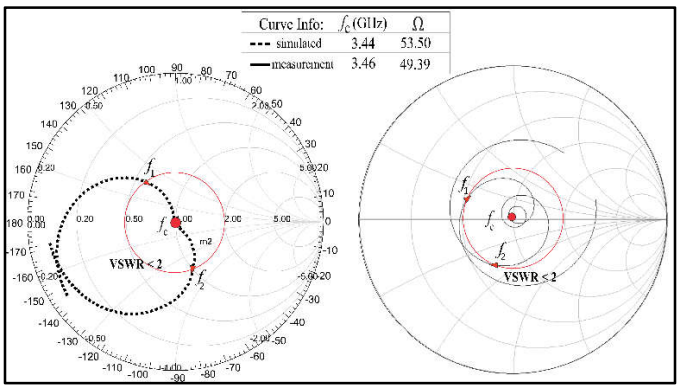

(b)

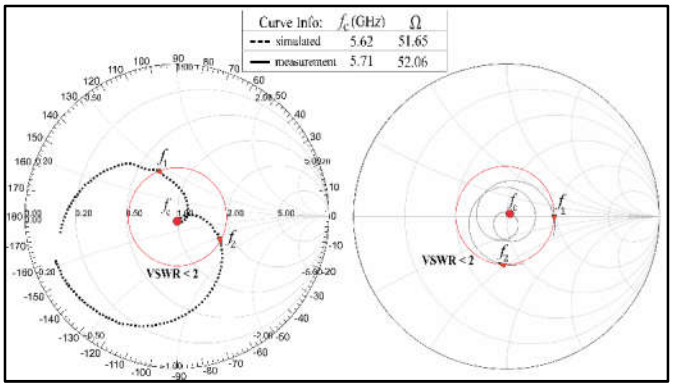

(c)

Figura 7. Impedances about the Smith chart's, simulated and measurement of the antennas: (a) MPA R1; (b) MPA R2; (c) MPA R3

Figure 7 shows simulated (left) and measured (right) impedances on the Smith Chart. From the results it can be observed that there is good matching impedance between transmission line and radiating element. The bands ($f_2 - f_1$) within the red curve indicated in the center of Smith's charts, both in the simulation and in the measurement, indicate the impedance bands with VSWR <2.

Table 2. Parameter values $|S_{11}|$ simulated and measured of the antennas, MPA R1, MPA R2 and MPA R3

Parameters	Analysis	MPA R1	MPA R2	MPA R3
	Simulated	2.39	3.44	5.63
f_c(GHz)	Measured	2.45	3.46	5.71
	Simulated	2.33	3.35	5.37
f_1(GHz)	Measured	2.36	3.40	5.48
	Simulated	2.44	3.53	5.75
f_2(GHz)	Measured	2.49	3.62	5.92
	Simulated	111.25	180.00	382.50
BW(MHz)	Measured	135.00	220.00	440.00
	Simulated	−40.57	−40.85	−41.40
$\|S_{11}\|$(dB)	Measured	−28.90	−33.60	−31.98

Table 3. Simulated irradiation diagram parameters, 3-D and 2-D in the E-plane and H-plane of the antennas: MPA R1, MPA R2 and MPA R3

Parametric of irradiation	MPA R1	MPA R2	MPA R3
Gain 3-D (dBi)	6.07	6.67	6.37
Gain 2-D (dBi)	5.95	6.45	6.15
HPBW	54.00°	50.00°	53.00°
F/B (dB)	-0.59	-0.66	-0.72
$J_{máx}$(A/m^2)	7.14	16.28	16.10

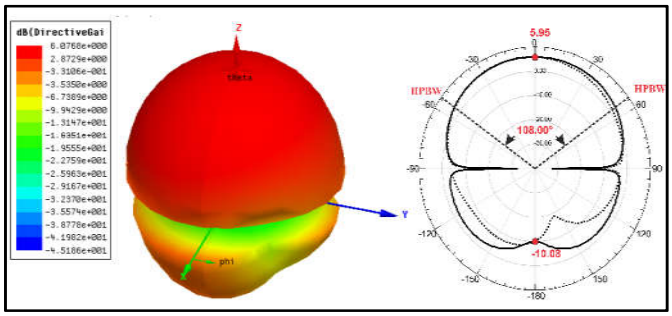

(a)

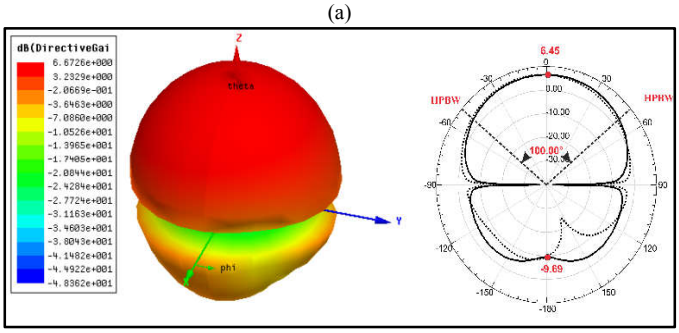

(b)

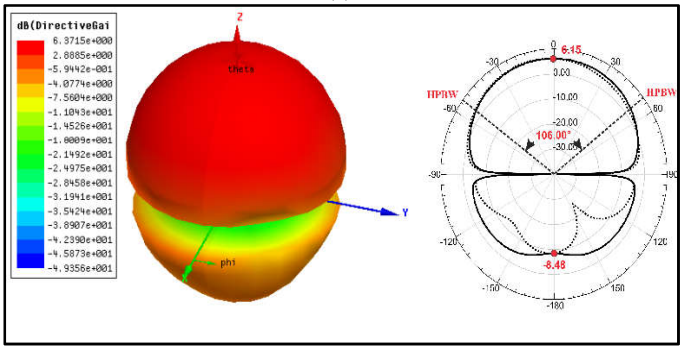

(c)

Figura 8. Simulated 3-D and 2-D irradiation diagrams of the antennas: (a) MPA R1, (b) MPA R2; (c) MPA R3

The larger the strip within this curve the greater the bandwidth of antenna impedance, in the case of measurements, it can be observed that the bandwidth of the antennas was greater than that of the simulated antennas. The 3-D and 2-D simulated radiation patterns of the MPA R1, MPA R2, and MPA R3 at in 2.39 GHz, 3.44 GHz, and 5.63 GHz antennas are illustrated in Figure 8, and the values of gain,half-power beam width (HPBW) and the front/back relationship (F/B), it can be observed in Table 3. The surface current density of the Riemann MPA R1, MPA R2, and MPA R3, simulated at 2.39 GHz, 3.44 GHz and 5.62 GHz, respectively, are illustrated in Figure 9. From these results, can be observed an increase in surface current density of the antennas MPA R2 and MPA R3, then corresponding to 16.28 A/m² and 16.10 A/m², in relation to the MPA R1 antenna which obtained 7.14 A/m², but without a significant difference in the total gain of the antennas, even with the reduction of the radiating element.

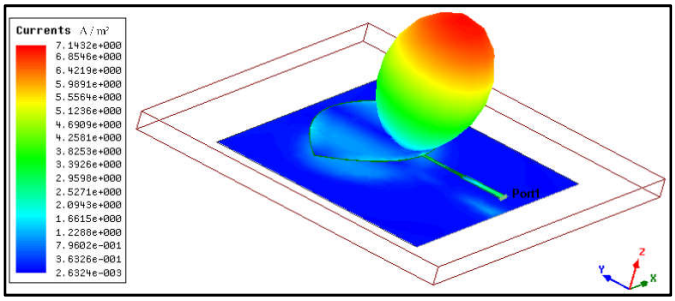

(a)

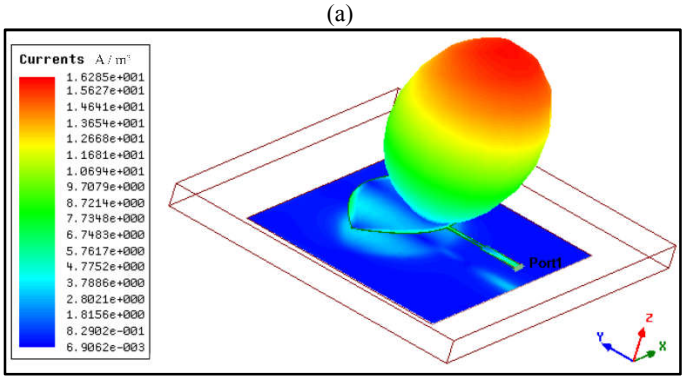

(b)

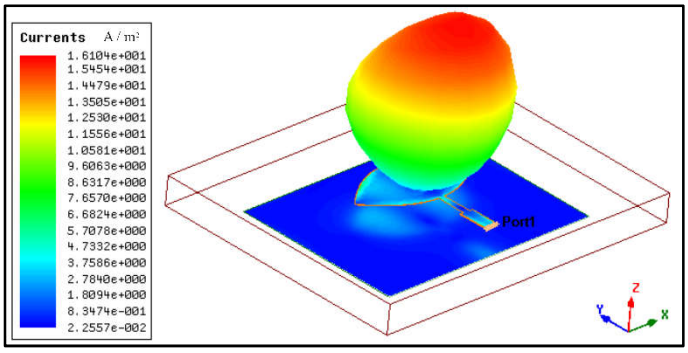

(c)

Figura 9. Surface current density distribution in (A / m2) and the distant field of the antennas: (a) MPA R1, (b) MPA R2, (c) MPA R3

Final Considerations: In this work was developed broadband patch antennas with the bio-inspired shape of the elliptical leaf using Riemann conformal transformation, on the square in the Argand-Gauss plane for wireless local area network (2.4 GHz and 5 GHz), and 5G band in 3.5 GHz. The project of the prototypes of the Riemann patch antennas presented an increase of the bandwidth of the narrowband antenna, with fractional bandwidth greater than 5%, increase in current density and gain constant, greater of 6 dBi.

Acknowledgements

The authors thank the support of GEMCA Group, State University of Paraíba (UEPB), Federal Institute of Paraíba (IFPB), and FAPESQ by financial support.

REFERENCES

Ajay, S. Gupta, S. C. Review and survey of broadband microstrip patch antennas. 2012. *International Journal of Computer Applications* (0975 - 8887). vol. 59 No. 10, Decembrer 2012.

Aravindraj, E. and Ayyappan,K. "Design of slotted H-shaped patch antenna for 2.4 GHz WLAN applications," 2017 *International Conference on Computer Communication and Informatics* (ICCCI), Coimbatore, 2017, pp. 1-5.doi: 10.1109/ICCCI.2017.8117773.

Ata, O. W. Salamin, M. and Abusabha, K. "Double U-Slot Rectangular Patch Antenna for Multiband Applications," 2018 *International Symposium on Advanced Electrical and Communication Technologies* (ISAECT), Rabat, Morocco, 2018, pp. 1-6. doi: 10.1109/ISAECT. 2018.8618855.

Balanis, C. A. Antenna Theory: Analysis and desing. 2° edição. Canada: John Wiley & Sons, 1997.

Chen, Z. N. and Chia, M. Y. W. Broadband Planar Antennas: Design and Applications. Singapore, John Wiley & Sons, pp. 17-19, 2005.

Deschamps, A. G. Microstrip Microwave Antenas. Presented at the Third USAF Symposium on Antennas, 1953.

Deshmukh, A. A. Jain, A. R. and Ray, K. P. "Broadband rectangular slot cut modified circular microstrip antenna," 2013 Annual IEEE India Conference (INDICON), Mumbai, 2013, pp. 1-5. doi: 10.1109/INDCON.2013. 6725953.

Ibrahim, M. S. "Low-Cost, Circularly Polarized, and Wideband U-Slot Microstrip Patch Antenna with Parasitic Elements for WiGig and WPAN Applications," 2019 13th European Conference on Antennas and Propagation (EuCAP), Krakow, Poland, 2019, pp. 1-4.

Jeffrey, C. S. Kufre, M. U. Akaninyene, B. O. Compact Rectangular Slot Patch Antenna for Dual Frequency Operation Using Inset Feed Technique, *International Journal of Information and Communication Sciences*. Vol. 1, No. 3, 2016, pp. 47-53. doi: 10.11648/j.ijics. 20160103.13.

Jui-Han Lu, "Broadband dual-frequency operation of circular patch antennas and arrays with a pair of L-shaped slots," in IEEE Transactions on Antennas and Propagation, vol. 51, no. 5, pp. 1018-1023, May 2003.doi: 10.1109/TAP. 2003.811477.

Khan, M. and Chatterjee, D. "Analysis of Reactive Loading in a U-Slot Microstrip Patch Using the Theory of Characteristic Modes [Antenna Applications Corner]," in *IEEE Antennas and Propagation Magazine,* vol. 60, no. 6, pp. 88-97, Dec. 2018. doi: 10.1109/MAP.2018.2870653.

Khidre, A. Lee, K. Elsherbeni, A. Z. and Yang, F. "Wide Band Dual-Beam U-Slot Microstrip Antenna," in IEEE Transactions on Antennas and Propagation, vol. 61, no. 3,

pp. 1415-1418, March 2013. doi: 10.1109/TAP.2012. 2228617.

Kumar, G. and Ray, K. P. Broadband Microstrip Antennas. London, Artech House, 2003. IBSN: 1-58053-244-6.

Nitin, N. Agrawal, N. Siddiqui, M. G. and Ansari, J. A. "Design and Analysis of E-Slot Microstrip Antenna," 2018 Recent Advances on Engineering, Technology and Computational Sciences (RAETCS), Allahabad, 2018, pp. 1-5.doi: 10.1109/RAETCS.2018.8443948.

Silva Junior, P. F, Silva Pinto, M. S., Santana, E. E. C., Silva, P. H. F. S., Oliveira, E. E. C., Oliveria, M. A., Batista, F. F., Serres, A. J. R., Freire, R. C. S., Neto, A. S. S., Neto, S. A. A., Cruz, C. A. M. Fractal and Polar Microstrip Antennas and Arrays for Wireless Communications. In: Wireless Mesh Networks. IntechOpen. DOI: 10.5772/ intechopen.83401.

Silva Junior, P. F., Freire, R. C.S., Serres, A. J. R., Catunda, S. Y., Silva, P. H.F. Bioinspired transparent antenna for WLAN application in 5 GHz.MicrowOpt Technol Lett. 2017, vol. 59, pp. 2879–2884. DOI: 10.1002/mop.30853

Silva Junior, P. F., Santana, E. E. C., P. F, Silva Pinto, M. S., Silva, P. H. F. S., Albuquerque, C. C. R., Serres, A. J. R., Freire, R. C. S. Bio-Inspired On-Chip Antenna Array for ISM Band 60 GHz Application. Journal of Integrated Circuits and Systems, vol. 14, n. 2, 2019. DOI: 10.29292/jics.v14i2.53

Silva Junior, P. F., Serres, A. J. R., Freire, R. C. S., Serres, G. K. F., Gurjão, E C., Carvalho, J. N., Santana, E. E. C. Bio-Inspired Wearable Antennas, Wearable Technologies, Intech Open, DOI: 10.5772/intechopen.75912.

Silva Junior, P. F., Silva, P. H. F., Serres, A. J. R., Silva, J. C., Freire, R. C. S. Design of directional Leaf-shaped printed monopole antennas for 4G 700 MHz band. MicrowOpt Technol Lett. 2017, vol. 58, pp. 1529–1533. DOI: 10.1002/mop.29853.

Silva Junior, P.F., Freire, R.C.S., Serres, A.J.R., Silva, P.H.F., Silva, J.C. Wearable textile bioinspired antenna for 2G, 3G, and 4G systems. Microw. Opt. Technol. Lett., vol.58, 2016, pp. 2818-2823. doi:10.1002/mop.30150.

Stuzman,W. L, Gary, A. Thiele. Antenna theory and design. 3rd ed. Wiley, 2013. IBSN: 978-0-470-57664-9.

****